

Multicomponent magneto-orbital order and magneto-orbitons in monolayer VCl_3

Luigi Camerano,¹ Adolfo O. Fumega,² Gianni Profeta,^{1,3} and Jose L. Lado²

¹*Department of Physical and Chemical Sciences,
University of L'Aquila, Via Vetoio, 67100 L'Aquila, Italy*

²*Department of Applied Physics, Aalto University, 02150 Espoo, Finland*

³*CNR-SPIN L'Aquila, Via Vetoio, 67100 L'Aquila, Italy*

Van der Waals monolayers featuring magnetic states provide a fundamental building block for artificial quantum matter. Here, we establish the emergence of a multicomponent ground state featuring magneto-orbital excitations of the $3d^2$ -transition metal trihalide VCl_3 monolayer. We show that monolayer VCl_3 realizes a ground state with simultaneous magnetic and orbital ordering using density functional theory. Using first-principles methods we derive an effective Hamiltonian with intertwined spin and orbital degree of freedom, which we demonstrate can be tuned by strain. We show that magneto-orbitons appear as the collective modes of this complex order, and arise from coupled orbiton magnon excitations due to the magneto-orbital coupling in the system. Our results establish VCl_3 as a promising 2D material to observe emergent magneto-orbital excitations and provide a platform for multicomponent symmetry breaking.

Correlations in van der Waals materials represent the driving force behind a variety of unconventional electronic states, including unconventional superconductivity [1–3], exotic magnetism [4], and fractional topological states [5, 6]. Van der Waals magnetic materials [7, 8] provide a highly tunable platform to engineer a variety of quantum states, including ferromagnetism in CrBr_3 and CrI_3 [9, 10], antiferromagnetism in FePS_3 [11], heavy-fermion Kondo states in CeSiI [12, 13] and in dichalcogenide bilayers [14–16], quantum spin liquid candidates in RuCl_3 [17, 18], 1T-TaSe₂ [19] and NbSe₂ [20], orbital magnets in twisted graphene bilayers [4, 21] and dichalcogenide bilayers [6, 22], and multiferroic order in NiI_2 [23, 24] and twisted CrBr_3 bilayers [25–28]. Among them, multiferroic materials feature, besides a magnetic order in the spin degree of freedom, an additional electronic ordering in a spatial degree of freedom. While multiferroic monolayers as NiI_2 [23, 24, 29–32] feature simultaneous magnetism and ferroelectricity, a variety of other multicomponent orders are potentially possible, in particular associated with an electronic reorganization in an internal orbitals degree of freedom [33].

Among van der Waals magnets, VCl_3 provides an ideal playground for complex electronic ordering due to the existence of orbital degeneracy leading to different potentially competing ground states [34]. VCl_3 belongs to family of vanadium trihalide materials, magnetic insulators due to its partially filled d-shell and strong correlations [35–41]. Orbital ordering in monolayers provides a unique platform to stabilize exotic multicomponent orders tunable via substrate [42] electric gate [43] or twist engineering, in contrast with the more challenging control of orbital order in bulk compounds [33, 44–47]. VCl_3 is an ideal candidate for orbital order due to its weaker spin-orbit coupling, which often quenches orbital order in heavier halides.

Here, we establish emergence of a multicomponent ordering in VCl_3 , featuring antiferro-orbital ordering coupled to a coexisting magnetic phase. Using first principles methods, we show that the orbital degeneracy in VCl_3

gives rise to different magnetic and orbital orderings, with the lowest energy configuration tunable by an external strain. We further show that these two orders are not independent, but strongly coupled, leading to strong magneto-orbital effects. This coupling gives rise to the appearance of new hybrid quasiparticles emerging from magnons and orbital excitations. Our results establish VCl_3 as a paradigmatic material to realize multiferroic orbital ordering, providing a van der Waals monolayer enabling the observation magneto-orbital excitations.

We first address the electronic structure of VCl_3 in the monolayer limit. VCl_3 hosts 2 electrons in the three-fold t_{2g} manifold in an octahedral environment O_h (see Fig. 1a) similar to those observed in ABO_3 perovskites [44–47]. Due to partial occupation of d orbitals in t_{2g} shell, a Jahn-Teller distortion [48] of the octahedra lowers the symmetry from O_h to trigonal point group D_{3d} (see Fig. 1a), splitting the t_{2g} manifold in a singlet a_{1g} and a doublet e'_g . Spontaneous symmetry breaking leads to a further splitting of the e'_g manifold lifting the orbital degeneracy. The occupation of these two nearly-degenerate states for each V atoms gives rise to orbital ordered phases, which can have a ferro-orbital (FO) (all the V atoms are in the same orbital configuration) or anti-ferro orbital (AFO) (nearest-neighbours V atoms are in different orbital configuration) phases. First-principles DFT+ U method ($U = 3.2$ eV) yield a symmetry broken orbitally ordered phases, always favored in energy with respect to both the $a_{1g}^1 e'_g^1$ metallic phase and the e'_g^2 insulating phase. These orbitally ordered phases are stabilized by strong correlation, as clear from its evolution as a function of the U parameter. As DFT calculations feature a competition between electronic and magnetic degree of freedom [34], the convergence of the orbital ordered phases in a DFT+ U framework is particularly challenging and requires a symmetry unconstrained unit cell and the use of the d -density matrix occupation control. By its suitable initial guesses we compute both FO and AFO ordered phases whose magnetization densities are reported in Fig. 1b. In the case of orbital order phases

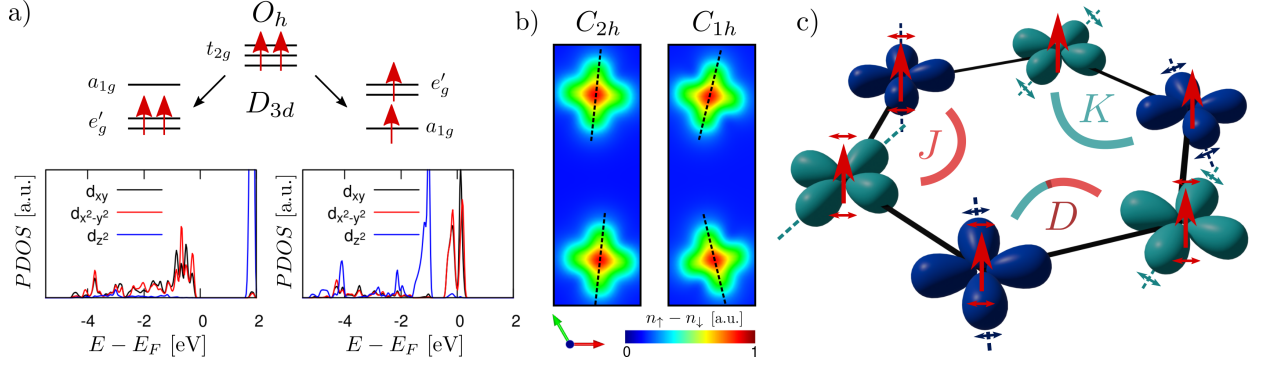


FIG. 1. a) Schematic representation of the V- d orbitals in an octahedral environment (O_h) and two possible electronic configuration after trigonal distortion (D_{3d}). The corresponding DFT+ U density of state projected on V- d is reported in the lower panel showing orbital order states. b) First principle calculated magnetization density ($n_\uparrow - n_\downarrow$) in the case of ferromagnetic ferro-orbital (C_{2h} symmetry) and ferromagnetic antiferro-orbital (C_{1h} symmetry). c) Sketch of the model presented in this study, the different colors for the orbitals highlight different V-sites in the antiferro-orbital phase. The coupling constant J , K , D , are referred to the model in Eq. (1).

the electronic instability is followed by a different lowering of the crystal symmetry (from D_{3d} to C_{2h} for the FO and to C_{1h} for the AFO). It is worth noting how in the case of AFO the inversion symmetry of the honeycomb lattice is broken, possibly inducing a non-zero charge polarization. Comparing the energy of the FO and AFO we find that the AFO phase is favored, meaning that the ground state of the system is the AFO ferromagnetic phase. In order to study the stability of this solution for a wide range of structural parameters, we applied in-plane strain to the lattice, finding that the AFO phase always remains stable. The orbital ordering mechanism can be directly visualized from the density of states on vanadium d_{z^2} , d_{xy} and $d_{x^2-y^2}$ [49] showing the different occupation of the in-plane d_{xy} and $d_{x^2-y^2}$ orbitals in the AFO phase but the same occupation of the d_{z^2} orbital. The orbitally ordered phases in a magnetic van der Waals material give rise to a multicomponent ordering, which, if coupled can further stabilizes composite excitations. We address this possibility by deriving a model Hamiltonian from the converged first principle phases, using a spin \vec{S} and pseudo-spin τ^z (describing the orbital configuration) operators to uncover the possible interaction between spin and orbital degree of freedom.

The multiple degrees of freedom renders VCl_3 a material realizing an effective $SU(4) = SU(2)_{\text{spin}} \times SU(2)_{\text{orbital}}$ model, similar to flat bands of twisted graphene multilayers [50–56]. In the orbital degree of freedom, $SU(2)_{\text{orbital}}$ symmetry is broken into a $U(1)_{\text{orbital}}$ symmetry due to the crystal lattice, in analogy with the valley degree of freedom in twisted graphene multilayers. Using first principles calculations we can map the effective Hamiltonian in the spin and orbital degrees of freedom [57], that takes the form

$$H = -\frac{J}{2} \sum_{\langle ij \rangle} \vec{S}_i \cdot \vec{S}_j - \frac{K}{2} \sum_{\langle ij \rangle} \tau_i^z \tau_j^z - \frac{D}{2} \sum_{\langle ij \rangle} \vec{S}_i \cdot \vec{S}_j \tau_i^z \tau_j^z \quad (1)$$

where $\langle \rangle$ denotes first vanadium neighbors, J is the isotropic Heisenberg-like coupling, K is the anisotropic Ising-like coupling between pseudo-spins and D represent the coupling between the spin and pseudo-spin variables. Since VCl_3 hosts two electrons in an high spin configuration, $S = 1$, while the pseudo-spin can be described by an Ising coupling with $\tau^z = \frac{1}{2}$. Thus, K capture the orbital exchange interaction while D the coupling with the spin degree of freedom. The schematic of this model is shown in Fig. 1c. We take in Eq. (1) that there is a strong easy axis for the pseudospin, associated with the explicit breaking of $SU(2)_{\text{orbital}}$ due to the lattice. This assumption is justified by our first-principles calculation, which converges to the same orbital configuration shown in Fig. 1b, even when the d -density matrix is initialized with rotated axes. Depending on the values of J , K and D different spin-orbital orders emerge from this model [58–60]. By ab-initio calculation, we calculated the effective parameters present in the Hamiltonian (1) through the stabilization of four possible ground states: (I) FO-FM, (II) FO-AFM, (III) AFO-FM, (IV) AFO-AFM (see Fig. 2a), where FM and AFM stands for ferromagnetic and antiferromagnetic respectively. We treat equation (1) in the classical approximation, i.e. describing spins \vec{S} as dimensionless classical vectors of length S in the sphere and considering $\tau_i^z \tau_j^z = \pm 1$. We denote the corresponding ground state energies as $\epsilon_{FO,FM}$, $\epsilon_{FO,AFM}$, $\epsilon_{AFO,FM}$ and $\epsilon_{AFO,AFM}$. The spin-orbital model allows to write the energy per unit cell (honeycomb lattice 2 V atoms) of the different configurations as [61] $\epsilon_{FO,FM} = -3JS^2 - 3K^2 - 3D^2S^2 + E_0$, where E_0 is a constant energy term. In order to determine J , K and D , we use the ground state energies for these 4 configurations as obtained from our DFT calculations. The obtained results are reported in Fig. 2b-c-d as a function of the lattice parameter a and for different values of the Hubbard U . We note that the theoretical lattice constant at the DFT+ U level is $a = 6.24$ Å to be compared with

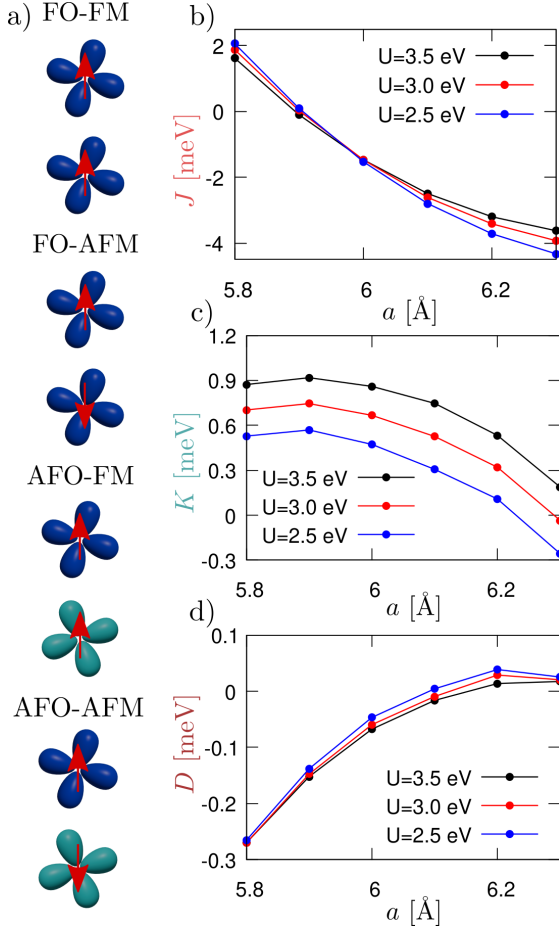


FIG. 2. a) Schematic representation of the 4 states (see the main manuscript) that are needed to calculate the exchange coupling of the model. b), c) and d) Isotropic Heisenberg coupling (J), anisotropic orbital exchange coupling (K) and spin-orbital coupling (D) as a function of the lattice parameter a for different values of the Hubbard repulsion U .

available experimental lattice parameter for the bulk is $a = 6.01$ Å [62]. In general, we find $J > K \gg D$, however, depending on the strain, the spin-orbital coupling D can be enhanced by one order of magnitude. With $a = 5.80$ Å, close to the experimental bulk lattice parameter, $D = -0.27$ meV independently on the U value. It is worth noting that the exchange orbital coupling K is highly dependent on the value of U . This aligns with the scenario where correlation effects drive the orbital ordering. Specifically, higher U values result in stronger orbital coupling, while in the limit of small U , the orbital coupling is quenched. Another important feature is the dependence of the spin exchange coupling J on lattice strain, where at some strains the coupling switches from ferromagnetic to antiferromagnetic. This phenomenology may account for the significant impact of the substrate on the magnetic order, as recently demonstrated in Ref. [42]. This allows for strain engineering of the magnetism, which in this material is coupled with the

orbital and consequently the charge degrees of freedom. Finally, we note how for $a = 5.9$ Å, J is almost quenched while D is enhanced. In this regime, controlling the orbital configuration permits to switch from ferromagnetic to antiferromagnetic phase and viceversa. Thus, the first principle mapping on the Hamiltonian in Eq. (1) reveals a sizable coupling between spin and orbital degrees of freedom in VCl_3 .

The magnetic and orbital orders breaking gives rise to magnetic and orbital excitations which can be studied using the the Hamiltonian in Eq. (1). Considering only the spin degree of freedom, gapless magnons will arise due to the continuous symmetry of the spin sector. Due to the 2D nature of the magnetism, magnetic anisotropy is necessary for magnetic order to occur. We do not include it in our model, as it does not influence the magnon dispersion aside from opening a small magnon gap [10]. Orbital excitations will have a gapped spectra due to the Ising-like interaction considered. To study elementary excitation we can consider Hamiltonian (1) as composed $H = H_s + H_o + H_{int}$, where H_s is the only spin Hamiltonian, H_o the orbital one and H_{int} is the interaction term proportional to D . H_s and H_o are studied in terms of linear spin waves (LSW) and linear orbital waves (LOW) [63–65]. We perform first an Holstein-Primakoff transformation introduce bosonic operators b_i and α_i ($\tau_i^z = \tau^z - b_i^\dagger b_i$, $S_i^z = S - \alpha_i^\dagger \alpha_i$, $S_i^+ = \sqrt{2S} \alpha_i$, $S_i^- = \sqrt{2S} \alpha_i^\dagger$ for the ferromagnetic case), then a Bogoliubov transformation gives the magnon dispersion and introduce magnon creation and annihilation operators a_i^\dagger, a_i . When the spin-orbital coupling is considered via H_{int} , the full Hamiltonian H becomes biquadratic and a decoupling [66, 67] is performed. By introducing a spin-orbital hybridization function and neglecting the anomalous terms, we can write down the effective Hamiltonian H_{eff} as

$$H_{eff} = \sum_{\nu, \mathbf{k}} \omega_\nu(\mathbf{k}) a_{\mathbf{k}, \nu}^\dagger a_{\mathbf{k}, \nu} + \sum_{\mathbf{k}} \omega_o(\mathbf{k}) b_{\mathbf{k}}^\dagger b_{\mathbf{k}} + \sum_{\nu, \mathbf{k}} \gamma^\nu(\mathbf{k}) a_{\mathbf{k}, \nu}^\dagger b_{\mathbf{k}} + h.c. \quad (2)$$

where $a_{\mathbf{k}, \nu}^\dagger$ $b_{\mathbf{k}}^\dagger$ are bosonic operators which create a magnon with energy $\omega_\nu(\mathbf{k})$ in the magnon band ν and an orbiton with energy $\omega_o(\mathbf{k})$ respectively. The spin-orbital hybridization function depends on the magneto-orbital coupling as $\gamma^\nu(\mathbf{k}) \sim D \langle a_{\mathbf{k}} b_{\mathbf{k}}^\dagger \rangle$. $\omega_o(\mathbf{k})$ is the analogous of $\omega_\nu(\mathbf{k})$ for the magnons, but in our Hamiltonian (1), due to the Ising-like interaction between pseudospins, $\omega_o(\mathbf{k}) = 6K$. If we consider the possibility of orbital in-plane rotation or a bond-dependent coupling, $\omega_o(\mathbf{k})$ could depend on \mathbf{k} resulting in an orbital excitation dispersion. Finally, the magneto-orbital coupling also renormalizes the exchange spin and orbital interaction, as shown by rewriting Eq. (1) in the following form $H = \sum_{\langle i, j \rangle} J_{ij} (\vec{S}_i \cdot \vec{S}_j + 1)$ where $J_{ij} = J_{ij}(\tau_i^z, \tau_j^z)$ [68].

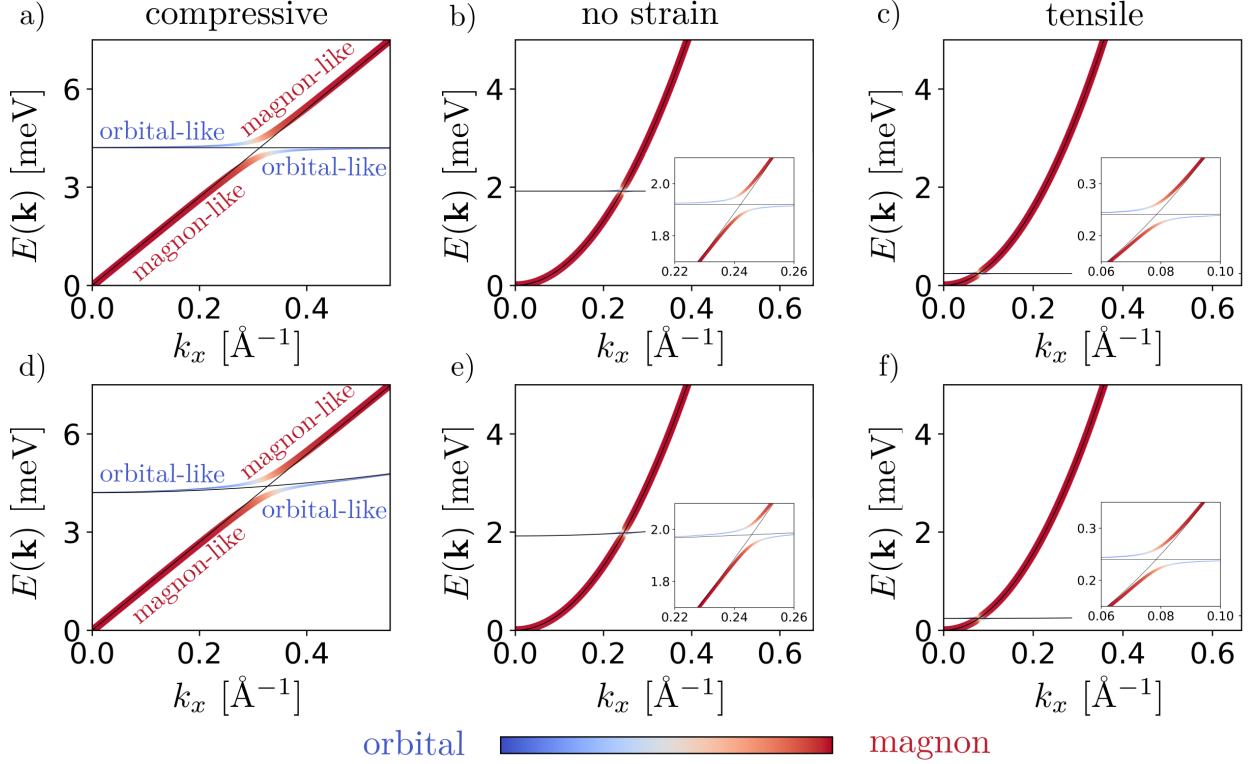


FIG. 3. Magnon-orbital excitation as a function of the strain. In particular in a), b) and c) the excitation spectra are reported for the coupling values reported in Fig. 2. In d), e) and f) a \mathbf{k} dispersion for the orbital excitation is assumed ($\omega_o(\mathbf{k})$), representing the coupling with other orbitals (see main text). The color bar represent the excitation character and the linewidth is proportional to the projection on magnon manifold. The black thin lines represent the magnon and orbital dispersion without hybridization ($D = 0$).

The Hamiltonian (2) is solved by expanding the Hilbert space of the spin states (first term in Eq. (2)) to include the pseudo-spins (second term in (2)) and their hybridization with spins (third term in (2)). Since $J > K$ we expand the magnon and orbital dispersion near the Γ point. In this limit, ferromagnetic dispersion is parabolic with an effective mass $m_{eff,S} = \frac{1}{4}JSa^2$ while antiferromagnetic dispersion is linear with an effective velocity $v_{eff} = \sqrt{\frac{3}{2}}JSa$ in an honeycomb lattice. The results of the entangled magnon and orbital spectrum are summarized in Fig. 3 as a function of the strain. We first consider the case of the Hamiltonian (1), in which orbitals cannot rotate 3a-b-c. In absence of spin-orbital hybridization ($D = 0$), the spectra consist into two different dispersions, $\omega_\nu(\mathbf{k})$ and $\omega_o(\mathbf{k})$, which do not interact. In the presence of magneto-orbital coupling ($D \neq 0$), a gap appears in the magnon spectrum, with its amplitude proportional to the coupling. Moreover, magnons and orbitons hybridize at the crossing points opening a gap giving rise to magnon-orbital excitations (Fig. 3). Thus, the multicomponent order gives rise to both orbiton excitations as the one detected in Ref. [69] and hybridized magnon-orbital excitations which, at the best of our knowledge, have never been experimentally observed. In Fig. 3d-e-f we consider the general case in which the

interaction between orbital is of the type $\vec{\tau}_i^{(\gamma)} K_{ij}^{(\gamma)} \vec{\tau}_j^{(\gamma)}$, i.e. the pseudo-spin interaction allows both in-plane rotation and bond-dependent (γ) coupling. This leads to the emergence of an orbital dispersion $\omega_o(\mathbf{k})$ [66–68]. In this case the dispersion is not linear due to the strong anisotropy that describes the pseudo-spin variable. In order to verify if the energy gap is preserved including orbital dispersion, we consider an orbiton dispersion with an effective mass $m_{eff,O} = K_\perp \tau^z a^2$ where $K_\perp \simeq \frac{1}{16}K$ as estimated in Ref. [68]. The main consequence of $\omega_o(\mathbf{k})$ is the tilting of the magnon bands at the points where the magnon and orbiton bands intersect, still showing the presence of a gap. This effect becomes more pronounced as the orbital coupling increases (see Fig. 3d). Another consequence of the general pseudo-spin interaction, which we do not explore in this work but is worth mentioning, is the emergence of a Kitaev-like interaction between spins in the limit of strong SOC [70, 71]. This is not the case for VCl_3 due to the lighter halide, but it could be the case for VI_3 if entangled magneto-orbital ordered phases can also be stabilized in this compound. Finally, we show how the amplitude of the gap and the strength of the hybridization can be tuned by in-plane strain. In particular, for a relatively large 6% compressive strain (Fig. 3a-d) the system is an antiferromagnet with a very large magneto-orbital coupling ($D = -0.27$

meV) due to the increased hybridization, but only a 0.2% tensile strain strongly decreases the orbital exchange coupling eventually causing it to disappear [72].

Here we show that VCl_3 develops multiferroic order in both the orbital and spin degrees of freedom, giving rise to intertwined magnon and orbital excitations. Through first-principles calculations, we establish the appearance of strain-dependent ferro- and antiferro-orbital ordered phases in VCl_3 , coexisting with the magnetic state. Based on first-principles methods, we derived a low-energy Hamiltonian that accounts for the magnon and orbital excitations, including the effect of magneto-orbital coupling between both degrees of freedom. The magneto-orbital coupling gives rise to magneto-orbital excitations stemming from the multicomponent order, establishing an exotic excitation that can be probed in this monolayer material. We show that magneto-orbital coupling, orbital order, and magnetic order are tunable with strain, making VCl_3 a potential platform for magneto-orbital straintronics. In particular, inhomoge-

neous strain, such as that present in twisted heterostructures, is expected to give rise to moiré domains with different magneto-orbital ordering and magneto-orbital dynamics, providing a new playground in moiré matter. Our results establish the deep interplay between orbital and magnetic ordering in VCl_3 , presenting a paradigmatic example of a multicomponent ordered phase in van der Waals materials.

Acknowledgements- G.P. acknowledges the European Union-NextGenerationEU under the Italian Ministry of University and Research (MUR) National Innovation Ecosystem Grant No. ECS00000041 VITALITY-CUP E13C22001060006 for funding the project. G.P. and L.C. acknowledge support from CINECA Supercomputing Center through the ISCR project. J.L.L. and A.O.F. acknowledge the computational resources provided by the Aalto Science-IT project and the financial support from the Academy of Finland Projects Nos. 331342, 358088, and 349696, the Jane and Aatos Erkko Foundation, and the Finnish Quantum Flagship.

-
- [1] Jeong Min Park, Yuan Cao, Kenji Watanabe, Takashi Taniguchi, and Pablo Jarillo-Herrero, “Tunable strongly coupled superconductivity in magic-angle twisted trilayer graphene,” *Nature* **590**, 249–255 (2021).
 - [2] Yuan Cao, Jeong Min Park, Kenji Watanabe, Takashi Taniguchi, and Pablo Jarillo-Herrero, “Pauli-limit violation and re-entrant superconductivity in moiré graphene,” *Nature* **595**, 526–531 (2021).
 - [3] Hyunjin Kim, Youngjoon Choi, Cyprian Lewandowski, Alex Thomson, Yiran Zhang, Robert Polski, Kenji Watanabe, Takashi Taniguchi, Jason Alicea, and Stevan Nadj-Perge, “Evidence for unconventional superconductivity in twisted trilayer graphene,” *Nature* **606**, 494–500 (2022).
 - [4] M. Serlin, C. L. Tschirhart, H. Polshyn, Y. Zhang, J. Zhu, K. Watanabe, T. Taniguchi, L. Balents, and A. F. Young, “Intrinsic quantized anomalous hall effect in a moiré heterostructure,” *Science* **367**, 900–903 (2020).
 - [5] Jiaqi Cai, Eric Anderson, Chong Wang, Xiaowei Zhang, Xiaoyu Liu, William Holtzmann, Yinong Zhang, Fengren Fan, Takashi Taniguchi, Kenji Watanabe, Ying Ran, Ting Cao, Liang Fu, Di Xiao, Wang Yao, and Xiaodong Xu, “Signatures of fractional quantum anomalous hall states in twisted mote_2 ,” *Nature* **622**, 63–68 (2023).
 - [6] Fan Xu, Zheng Sun, Tongtong Jia, Chang Liu, Cheng Xu, Chushan Li, Yu Gu, Kenji Watanabe, Takashi Taniguchi, Bingbing Tong, Jinfeng Jia, Zhiwen Shi, Shengwei Jiang, Yang Zhang, Xiaoxue Liu, and Tingxin Li, “Observation of integer and fractional quantum anomalous hall effects in twisted bilayer mote_2 ,” *Phys. Rev. X* **13**, 031037 (2023).
 - [7] M. Gibertini, M. Koperski, A. F. Morpurgo, and K. S. Novoselov, “Magnetic 2d materials and heterostructures,” *Nature Nanotechnology* **14**, 408–419 (2019).
 - [8] M. Blei, J. L. Lado, Q. Song, D. Dey, O. Erten, V. Pardo, R. Comin, S. Tongay, and A. S. Botana, “Synthesis, engineering, and theory of 2d van der waals magnets,” *Applied Physics Reviews* **8** (2021), 10.1063/5.0025658.
 - [9] Bevin Huang, Genevieve Clark, Efrén Navarro-Moratalla, Dahlia R. Klein, Ran Cheng, Kyle L. Seyler, Ding Zhong, Emma Schmidgall, Michael A. McGuire, David H. Cobden, Wang Yao, Di Xiao, Pablo Jarillo-Herrero, and Xiaodong Xu, “Layer-dependent ferromagnetism in a van der waals crystal down to the monolayer limit,” *Nature* **546**, 270–273 (2017).
 - [10] J L Lado and J Fernández-Rossier, “On the origin of magnetic anisotropy in two dimensional cri_3 ,” *2D Materials* **4**, 035002 (2017).
 - [11] Jae-Ung Lee, Sungmin Lee, Ji Hoon Ryoo, Soonmin Kang, Tae Yun Kim, Pilkwang Kim, Cheol-Hwan Park, Je-Geun Park, and Hyeonsik Cheong, “Ising-type magnetic ordering in atomically thin fep_3s_3 ,” *Nano Letters* **16**, 7433–7438 (2016).
 - [12] Victoria A. Posey, Simon Turkel, Mehdi Rezaee, Aravind Devarakonda, Asish K. Kundu, Chin Shen Ong, Morgan Thinel, Daniel G. Chica, Rocco A. Vitalone, Ran Jing, Suheng Xu, David R. Needell, Elena Meirzadeh, Margalit L. Feuer, Apoorv Jindal, Xiaomeng Cui, Tonica Valla, Patrik Thunström, Turgut Yilmaz, Elio Vescovo, David Graf, Xiaoyang Zhu, Allen Scheie, Andrew F. May, Olle Eriksson, D. N. Basov, Cory R. Dean, Angel Rubio, Philip Kim, Michael E. Ziebel, Andrew J. Millis, Abhay N. Pasupathy, and Xavier Roy, “Two-dimensional heavy fermions in the van der waals metal cesii ,” *Nature* **625**, 483–488 (2024).
 - [13] Adolfo O. Fumega and Jose L. Lado, “Nature of the unconventional heavy-fermion kondo state in monolayer cesii ,” *Nano Letters* **24**, 4272–4278 (2024).
 - [14] Vilam Vaño, Mohammad Amini, Somesh C. Ganguli, Guangze Chen, Jose L. Lado, Shawulienu Kezilebieke, and Peter Liljeroth, “Artificial heavy fermions in a van der waals heterostructure,” *Nature* **599**, 582–586 (2021).
 - [15] Wen Wan, Rishav Harsh, Antonella Meninno, Paul Dreher, Sandra Sajan, Haojie Guo, Ion Errea, Fernando de Juan, and Miguel M. Ugeda, “Evidence for ground state coherence in a two-dimensional kondo lattice,” *Nature* **625**, 483–488 (2024).

- ture Communications **14** (2023), 10.1038/s41467-023-42803-4.
- [16] Wenjin Zhao, Bowen Shen, Zui Tao, Zhongdong Han, Kaifei Kang, Kenji Watanabe, Takashi Taniguchi, Kin Fai Mak, and Jie Shan, “Gate-tunable heavy fermions in a moiré kondo lattice,” *Nature* **616**, 61–65 (2023).
- [17] Arnab Banerjee, Jiaqiang Yan, Johannes Knolle, Craig A. Bridges, Matthew B. Stone, Mark D. Lumsden, David G. Mandrus, David A. Tennant, Roderich Moessner, and Stephen E. Nagler, “Neutron scattering in the proximate quantum spin liquid α -rucl 3,” *Science* **356**, 1055–1059 (2017).
- [18] Stephen M. Winter, Kira Riedl, David Kaib, Radu Coldea, and Roser Valentí, “Probing rucl₃ beyond magnetic order: Effects of temperature and magnetic field,” *Phys. Rev. Lett.* **120**, 077203 (2018).
- [19] Wei Ruan, Yi Chen, Shujie Tang, Jinwoong Hwang, Hsin-Zon Tsai, Ryan L. Lee, Meng Wu, Hyejin Ryu, Salman Kahn, Franklin Liou, Caihong Jia, Andrew Aikawa, Choongyu Hwang, Feng Wang, Yongseong Choi, Steven G. Louie, Patrick A. Lee, Zhi-Xun Shen, Sung-Kwan Mo, and Michael F. Crommie, “Evidence for quantum spin liquid behaviour in single-layer 1t-tase₂ from scanning tunnelling microscopy,” *Nature Physics* **17**, 1154–1161 (2021).
- [20] Quanzhen Zhang, Wen-Yu He, Yu Zhang, Yaoyao Chen, Lianguang Jia, Yanhui Hou, Hongyan Ji, Huixia Yang, Teng Zhang, Liwei Liu, Hong-Jun Gao, Thomas A. Jung, and Yeliang Wang, “Quantum spin liquid signatures in monolayer 1t-nbse₂,” *Nature Communications* **15** (2024), 10.1038/s41467-024-46612-1.
- [21] Jianpeng Liu and Xi Dai, “Theories for the correlated insulating states and quantum anomalous hall effect phenomena in twisted bilayer graphene,” *Phys. Rev. B* **103**, 035427 (2021).
- [22] Zui Tao, Bowen Shen, Shengwei Jiang, Tingxin Li, Lizhong Li, Liguang Ma, Wenjin Zhao, Jenny Hu, Kateryna Pistunova, Kenji Watanabe, Takashi Taniguchi, Tony F. Heinz, Kin Fai Mak, and Jie Shan, “Valley-coherent quantum anomalous hall state in ab-stacked mote₂/wse₂ bilayers,” *Phys. Rev. X* **14**, 011004 (2024).
- [23] Qian Song, Connor A. Occhialini, Emre Ergeçen, Batyr Ilyas, Danila Amoroso, Paolo Barone, Jesse Kapeghian, Kenji Watanabe, Takashi Taniguchi, Antia S. Botana, Silvia Picozzi, Nuh Gedik, and Riccardo Comin, “Evidence for a single-layer van der waals multiferroic,” *Nature* **602**, 601–605 (2022).
- [24] Mohammad Amini, Adolfo O. Fumega, Héctor González-Herrero, Viliam Vaňo, Shawulieny Kezilebieke, Jose L. Lado, and Peter Liljeroth, “Atomic-scale visualization of multiferroicity in monolayer nii₂,” *Advanced Materials* **36** (2024), 10.1002/adma.202311342.
- [25] Tiancheng Song, Qi-Chao Sun, Eric Anderson, Chong Wang, Jimin Qian, Takashi Taniguchi, Kenji Watanabe, Michael A. McGuire, Rainer Stöhr, Di Xiao, Ting Cao, Jörg Wrachtrup, and Xiaodong Xu, “Direct visualization of magnetic domains and moiré magnetism in twisted 2d magnets,” *Science* **374**, 1140–1144 (2021).
- [26] Hongchao Xie, Xiangpeng Luo, Zhipeng Ye, Zeliang Sun, Gaihua Ye, Suk Hyun Sung, Haiwen Ge, Shaohua Yan, Yang Fu, Shangjie Tian, Hechang Lei, Kai Sun, Robert Hovden, Rui He, and Liuyan Zhao, “Evidence of non-collinear spin texture in magnetic moiré superlattices,” *Nature Physics* **19**, 1150–1155 (2023).
- [27] Adolfo O Fumega and Jose L Lado, “Moiré-driven multiferroic order in twisted crcl₃, crbr₃ and cri₃ bilayers,” *2D Materials* **10**, 025026 (2023).
- [28] Shiva P. Poudel, Juan M. Marmolejo-Tejada, Joseph E. Roll, Martín A. Mosquera, and Salvador Barraza-Lopez, “Creating a three-dimensional intrinsic electric dipole on rotated cri₃ bilayers,” *Phys. Rev. B* **107**, 195128 (2023).
- [29] Adolfo O Fumega and J L Lado, “Microscopic origin of multiferroic order in monolayer nii₂,” *2D Materials* **9**, 025010 (2022).
- [30] Xuanyi Li, Changsong Xu, Boyu Liu, Xueyang Li, L. Bellaiche, and Hongjun Xiang, “Realistic spin model for multiferroic nii₂,” *Phys. Rev. Lett.* **131**, 036701 (2023).
- [31] Kira Riedl, Danila Amoroso, Steffen Backes, Aleksandar Razpopov, Thi Phuong Thao Nguyen, Kunihiko Yamauchi, Paolo Barone, Stephen M. Winter, Silvia Picozzi, and Roser Valentí, “Microscopic origin of magnetism in monolayer 3d transition metal dihalides,” *Phys. Rev. B* **106**, 035156 (2022).
- [32] Tiago V. C. Antão, Jose L. Lado, and Adolfo O. Fumega, “Electric field control of moiré skyrmion phases in twisted multiferroic NiI₂ bilayers,” *arXiv e-prints*, arXiv:2408.16600 (2024), arXiv:2408.16600 [cond-mat.str-el].
- [33] Y. Tokura and N. Nagaosa, “Orbital physics in transition-metal oxides,” *Science* **288**, 462–468 (2000).
- [34] Luigi Camerano and Gianni Profeta, “Symmetry breaking in vanadium trihalides,” *2D Materials* **11**, 025027 (2024).
- [35] Dario Matrippolito, Luigi Camerano, Hanna Swiatek, Bretislav Smid, Tomasz Klimczuk, Luca Ottaviano, and Gianni Profeta, “Polaronic and mott insulating phase of layered magnetic vanadium trihalide vcl₃,” *Phys. Rev. B* **108**, 045126 (2023).
- [36] Tai Kong, Karoline Stolze, Erik I. Timmons, Jing Tao, Danrui Ni, Shu Guo, Zoë Yang, Ruslan Prozorov, and Robert J. Cava, “Vi₃—a new layered ferromagnetic semiconductor,” *Advanced Materials* **31** (2019), 10.1002/adma.201808074.
- [37] Tai Kong, Shu Guo, Danrui Ni, and Robert J. Cava, “Crystal structure and magnetic properties of the layered van der waals compound VBr₃,” *Phys. Rev. Mater.* **3**, 084419 (2019).
- [38] Dávid Hovančík, Jiří Pospíšil, Karel Carva, Vladimír Sechovský, and Cinthia Piamonteze, “Large orbital magnetic moment in vi₃,” *Nano Letters* **23**, 1175–1180 (2023).
- [39] Ke Yang, Fengren Fan, Hongbo Wang, D. I. Khomskii, and Hua Wu, “vi₃: A two-dimensional ising ferromagnet,” *Phys. Rev. B* **101**, 100402 (2020).
- [40] Alessandro De Vita, Thao Thi Phuong Nguyen, Roberto Sant, Gian Marco Pierantozzi, Danila Amoroso, Chiara Bigi, Vincent Polewczyk, Giovanni Vinai, Loi T. Nguyen, Tai Kong, Jun Fujii, Ivana Vobornik, Nicholas B. Brookes, Giorgio Rossi, Robert J. Cava, Federico Mazzola, Kunihiko Yamauchi, Silvia Picozzi, and Giancarlo Panaccione, “Influence of orbital character on the ground state electronic properties in the van der waals transition metal iodides vi₃ and cri₃,” *Nano Letters* **22**, 7034–7041 (2022).
- [41] Derek Bergner, Tai Kong, Ping Ai, Daniel Eilbott, Claudia Fatuzzo, Samuel Ciocys, Nicholas Dale, Conrad Stansbury, Drew W. Latzke, Everardo Molina, Ryan

- Reno, Robert J. Cava, Alessandra Lanzara, and Claudia Ojeda-Aristizabal, “Polarization dependent photoemission as a probe of the magnetic ground state in the van der waals ferromagnet vi_3 ,” *Applied Physics Letters* **121** (2022), 10.1063/5.0108498.
- [42] Jinghao Deng, Deping Guo, Yao Wen, Shuangzan Lu, Zhengbo Cheng, Zemin Pan, Tao Jian, Yusong Bai, Hui Zhang, Wei Ji, Jun He, and Chendong Zhang, “Ferroelectricity in an antiferromagnetic vanadium trichloride monolayer,” (2024).
- [43] Bevin Huang, Genevieve Clark, Dahlia R. Klein, David MacNeill, Efrén Navarro-Moratalla, Kyle L. Seyler, Nathan Wilson, Michael A. McGuire, David H. Cobden, Di Xiao, Wang Yao, Pablo Jarillo-Herrero, and Xiaodong Xu, “Electrical control of 2d magnetism in bilayer cri_3 ,” *Nature Nanotechnology* **13**, 544–548 (2018).
- [44] M. Cwik, T. Lorenz, J. Baier, R. Müller, G. André, F. Bourée, F. Lichtenberg, A. Freimuth, R. Schmitz, E. Müller-Hartmann, and M. Braden, “Crystal and magnetic structure of latio_3 : evidence for nondegenerate t_{2g} orbitals,” *Phys. Rev. B* **68**, 060401 (2003).
- [45] Julien Varignon, Manuel Bibes, and Alex Zunger, “Origins versus fingerprints of the jahn-teller effect in d -electron abX_3 perovskites,” *Phys. Rev. Res.* **1**, 033131 (2019).
- [46] Zhi Wang, Oleksandr I. Malyi, Xingang Zhao, and Alex Zunger, “Mass enhancement in $3d$ and s - p perovskites from symmetry breaking,” *Phys. Rev. B* **103**, 165110 (2021).
- [47] Michael Marcus Schmitt, Yajun Zhang, Alain Mercy, and Philippe Ghosez, “Electron-lattice interplay in lamno_3 from canonical jahn-teller distortion notations,” *Phys. Rev. B* **101**, 214304 (2020).
- [48] Hermann Arthur Jahn and Edward Teller, “Stability of polyatomic molecules in degenerate electronic states—orbital degeneracy,” *Proceedings of the Royal Society of London. Series A-Mathematical and Physical Sciences* **161**, 220–235 (1937).
- [49] (), the d_{z^2} in global coordinates is the a_{1g} orbital in a trigonal symmetry, while the $d_{xy} \sim e'_{g,1}$ and $d_{x^2-y^2} \sim e'_{g,2}$ orbitals are a good representation of the e'_g manifold.
- [50] Dmitry V. Chichinadze, Laura Classen, Yuxuan Wang, and Andrey V. Chubukov, “ $\text{Su}(4)$ symmetry in twisted bilayer graphene: An itinerant perspective,” *Phys. Rev. Lett.* **128**, 227601 (2022).
- [51] M. Angeli, E. Tosatti, and M. Fabrizio, “Valley jahn-teller effect in twisted bilayer graphene,” *Phys. Rev. X* **9**, 041010 (2019).
- [52] Tobias M. R. Wolf, Oded Zilberberg, Gianni Blatter, and Jose L. Lado, “Spontaneous valley spirals in magnetically encapsulated twisted bilayer graphene,” *Phys. Rev. Lett.* **126**, 056803 (2021).
- [53] Mikito Koshino, Noah F. Q. Yuan, Takashi Koretsune, Masayuki Ochi, Kazuhiko Kuroki, and Liang Fu, “Maximally localized wannier orbitals and the extended hubbard model for twisted bilayer graphene,” *Phys. Rev. X* **8**, 031087 (2018).
- [54] Aline Ramires and Jose L. Lado, “Emulating heavy fermions in twisted trilayer graphene,” *Phys. Rev. Lett.* **127**, 026401 (2021).
- [55] Lasse Gresista, Dominik Kiese, Simon Trebst, and Michael M. Scherer, “Spin-valley magnetism on the triangular moiré lattice with $\text{su}(4)$ breaking interactions,” *Phys. Rev. B* **108**, 045102 (2023).
- [56] Y. H. Kwan, G. Wagner, T. Soejima, M. P. Zaletel, S. H. Simon, S. A. Parameswaran, and N. Bultinck, “Kekulé spiral order at all nonzero integer fillings in twisted bilayer graphene,” *Phys. Rev. X* **11**, 041063 (2021).
- [57] Kliment I Kugel’ and D I Khomskii, “The jahn-teller effect and magnetism: transition metal compounds,” *Soviet Physics Uspekhi* **25**, 231–256 (1982).
- [58] Philippe Corboz, Miklós Lajkó, Andreas M. Läuchli, Karlo Penc, and Frédéric Mila, “Spin-orbital quantum liquid on the honeycomb lattice,” *Physical Review X* **2** (2012), 10.1103/physrevx.2.041013.
- [59] Y. Tokura and N. Nagaosa, “Orbital physics in transition-metal oxides,” *Science* **288**, 462–468 (2000).
- [60] Jeroen van den Brink and Daniel Khomskii, “Double exchange via degenerate orbitals,” *Physical Review Letters* **82**, 1016–1019 (1999).
- [61] (), we only write down FO-FM phase for the sake of brevity.
- [62] Wilhelm Klemm and Ehrhard Krose, “Die kristallstrukturen von scl_3 , ticl_3 und vcl_3 ,” *Zeitschrift für anorganische Chemie* **253**, 218–225 (1947).
- [63] Minoru Takahashi, “Modified spin-wave theory of a square-lattice antiferromagnet,” *Physical Review B* **40**, 2494–2501 (1989).
- [64] Assa Auerbach, *Interacting Electrons and Quantum Magnetism* (Springer New York, 1994).
- [65] Krzysztof Wohlfeld, Andrzej M. Oleś, and Peter Horsch, “Orbitally induced string formation in the spin-orbital polarons,” *Physical Review B* **79** (2009), 10.1103/physrevb.79.224433.
- [66] O. Sikora and A. M. Oleś, “Spin and mixed spin-and-orbital excitations in kcu_3 ,” *physica status solidi (b)* **243**, 133–136 (2005).
- [67] Andrzej M. Oleś, Louis Felix Feiner, and Jan Zaanen, “Quantum melting of magnetic long-range order near orbital degeneracy: Classical phases and gaussian fluctuations,” *Physical Review B* **61**, 6257–6287 (2000).
- [68] G. Khaliullin and V. Oudovenko, “Spin and orbital excitation spectrum in the kugel-khomskii model,” *Physical Review B* **56**, R14243–R14246 (1997).
- [69] E. Saitoh, S. Okamoto, K. T. Takahashi, K. Tobe, K. Yamamoto, T. Kimura, S. Ishihara, S. Maekawa, and Y. Tokura, “Observation of orbital waves as elementary excitations in a solid,” *Nature* **410**, 180–183 (2001).
- [70] Akihisa Koga, Shiryu Nakauchi, and Joji Nasu, “Role of spin-orbit coupling in the kugel-khomskii model on the honeycomb lattice,” *Phys. Rev. B* **97**, 094427 (2018).
- [71] W. M. H. Natori, Hui-Ke Jin, and J. Knolle, “Quantum liquids of the $s = \frac{3}{2}$ kitaev honeycomb and related kugel-khomskii models,” *Phys. Rev. B* **108**, 075111 (2023).
- [72] For $a > 6.4\text{\AA}$ our first principles calculation cannot converge both FO and AFO phases.